Temporal trend in anthropogenic sulfur aerosol transport from central and eastern Europe to Israel

Arnon Karnieli,[1] Yevgeny Derimian,[1,2] Rodica Indoitu,[1] Natalya Panov,[1] Robert C. Levy,[3,4] Lorraine A. Remer,[3] Willy Maenhaut,[5] and Brent N. Holben[3]

Received 18 February 2009; revised 18 May 2009; accepted 28 May 2009; published 8 August 2009.

[1] Decrease of sulfur emissions in central and eastern Europe over the past 3 decades is well documented and linked to changes in economic activity, use of different fuels, addition of pollution controls, etc. These changes result in a decreasing trend of sulfate aerosol and aerosol forcing over the source region, but also at a receptor site located in southern Israel, thousands of kilometers downwind of the original source. A combination of several independent observations, namely, satellite and ground-based remote sensing, in situ aerosol sampling, and backward trajectory analysis, was implemented to show significant downward trends in fine particle aerosol optical thickness (AOT), in general, and sulfur aerosol, in particular, between 1995 and 2007. For the study years, MODIS-Terra observations over central and eastern Europe show 38% reduction of fine AOT. At the reception site in southern Israel, 43% reduction of fine AOT was observed by a ground-based sun/sky photometer and 25% reduction of sampled fine aerosols was obtained. During the corresponding observation periods, the coarse mode AOT has remained constant. The majority of the backward trajectories, where meaningful sulfur events were observed at the receptor site, are originated from eastern and central Europe. The aerosol radiative effect at top of the atmosphere has become less negative during the past decade, decreasing by 30% in Europe and 67% in Israel. The decrease in negative cloud-free aerosol forcing is consistent with observations of "global brightening" reported since 1990.

Citation: Karnieli, A., Y. Derimian, R. Indoitu, N. Panov, R. C. Levy, L. A. Remer, W. Maenhaut, and B. N. Holben (2009), Temporal trend in anthropogenic sulfur aerosol transport from central and eastern Europe to Israel, *J. Geophys. Res.*, *114*, D00D19, doi:10.1029/2009JD011870.

1. Introduction

[2] The element sulfur (S) (in its various forms or compounds) has been recognized as a major component of air pollution, acid rain, and processes that affect climate [e.g., *Kellogg et al.*, 1972]. Most of the atmospheric sulfur-related aerosols are formed by anthropogenic activities although there are minor sources of such particles in sea salt, gypsum, or other dust minerals [*Andreae and Rosenfeld*, 2008; *Myhre et al.*, 2004]. Coal and petroleum contain various amounts of sulfur compounds. Their combustion as fossil fuels in power plants, petroleum refineries, industry (e.g., for nonferrous smelting), and ground transportation generate sulfur dioxide (SO_2), and to lesser extent sulfur trioxide (SO_3), which are emitted into the atmosphere. In the atmosphere, SO_2 is quickly converted in a complex series of chemical reactions to sulfuric acid (H_2SO_4) and sulfate (SO_4^{2-}) aerosols [*Stockwell and Calvert*, 1983].

[3] The monthly conversion rates of SO_2 into sulfate aerosols are variable but generally, due to stronger solar radiation, photochemical processes responsible for the production of sulfate aerosols are enhanced during the summer [*Marmer et al.*, 2007; *Meagher et al.*, 1983]. The lifetime of sulfur in the atmosphere ranges from 12 h to 6 days [*Chin et al.*, 2000; *Chin and Jacob*, 1996]. Consequently, the sulfur-containing aerosols can be transported hundreds to thousands of kilometers downwind from their origin. Removal of the sulfur dioxide and sulfates (SO_x) from the atmosphere occurs by wet deposition (known as acid rain), diffusion of SO_2 to soil and vegetation, or dry deposition of sulfate particles [*Kellogg et al.*, 1972].

[4] For Europe as a whole, coal combustion gradually increased since the early 20th Century, becoming the dominant source of atmospheric sulfur by the end of the Second World War [*Mylona*, 1996]. In 1940, the annual emission of sulfur in Europe was estimated as 2.0×10^7 t a^{-1}. During the 1950s, sulfur emissions from liquid fuel combustion increased dramatically, so that by the 1970s, they were

[1]Remote Sensing Laboratory, Jacob Blaustein Institutes for Desert Research, Ben-Gurion University of the Negev, Sede Boker, Israel.
[2]Now at Laboratoire d'Optique Atmosphérique, Université de Lille, CNRS, Villeneuve d'Ascq, France.
[3]NASA Goddard Space Flight Center, Greenbelt, Maryland, USA.
[4]SSAI, Lanham, Maryland, USA.
[5]Department of Analytical Chemistry, Institute for Nuclear Sciences, Ghent University, Gent, Belgium.

Copyright 2009 by the American Geophysical Union.
0148-0227/09/2009JD011870

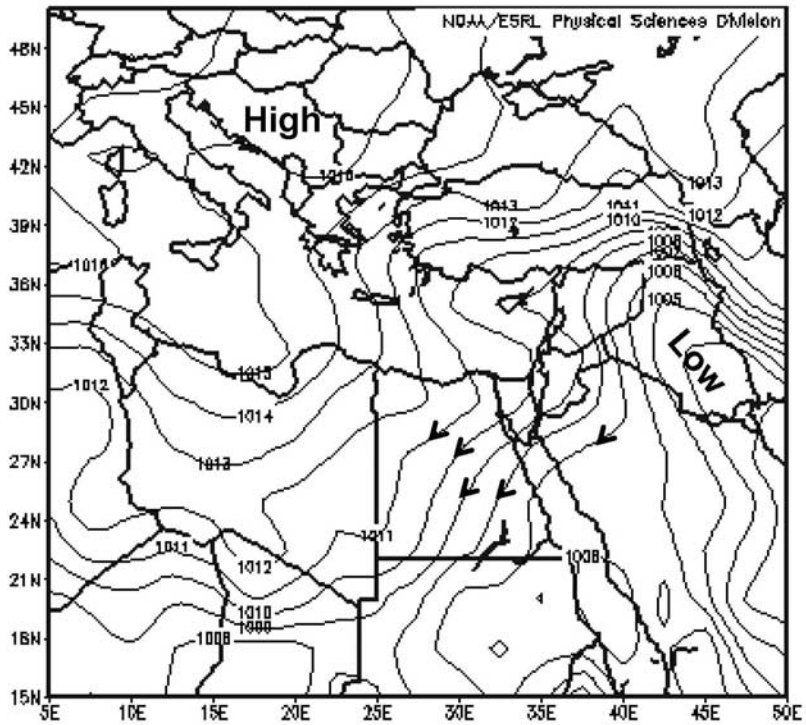

Figure 1. Long-term (1968–1996) average of sea level pressure for the summer season (May to September) over the research area (based on NCEP/NCAR Reanalysis data). The steep pressure gradient between the ridge in the northwest of the region and the Persian Trough in the southeast derives northwesterly winds that cause long-range transport of air masses carrying pollutants, from southeastern and southwestern Europe, into the eastern Mediterranean basin.

comparable to those from coal. The total sulfur emission reached a peak of 5.7×10^7 t a^{-1} in 1975. During the 1980s, western Europe experienced a marked decline in sulfur emission due to awareness of the health risks and environmental impacts that led to increasing use of alternative energy sources and less sulfurous fuels.

[5] A different situation took place in the member countries of the Soviet Bloc. As energy consumption per capita grew and prices of imported oil increased, these counties aspired for a self-sufficient energy supply. Consequently, central and eastern European countries mainly relied on lignite. Lignite is a brown coal, which requires extensive upgrading before it can be burned as a fuel source; therefore, it is a highly polluting material. Rapid economic growth of the former Soviet Bloc countries dominated any environmental concerns. Within the centrally controlled economies, energy-intensive industries (including iron, steel, light metals, chemicals, and engineering) were given priority, at the expense of efficient and low polluting energy production. After the collapse of the Soviet Union, central and eastern Europe reduced their economic activity and energy production, while also beginning to adapt policies of sulfur emission control. The consequence was that the region experienced a marked decline of sulfur emissions during the 1990s from $3.5\ 10^7 \times$ t a^{-1} in 1990 to 1.1×10^7 t a^{-1} in 2004 [*Vestreng et al.*, 2007].

[6] The sulfur emission trends of the last century are reflected in the changes of calculated radiative forcing. The magnitude of the monthly mean sulfate direct shortwave forcing at top of atmosphere increased from -0.6 W m^{-2} in July 1900 to -2.7 W m^{-2} in July 1980, and then it steadily decreased to -1.1 W m^{-2} in July 2000 [*Marmer et al.*, 2007]. These numbers represent the 24-h average change in net radiative flux at top of atmosphere due to the presence of sulfate aerosol during the summer season. Negatives indicate cooling of the Earth-atmosphere system. The net fluxes were calculated using a radiative transfer code, assumptions for sulfate aerosol optical properties, a sulfate distribution taken from a transport model simulation overlaid onto a map of surface albedos over Europe [*Marmer et al.*, 2007]. It should be noted that a decrease in emissions of 68% in Europe [*Vestreng et al.*, 2007] translates into a decrease of local negative forcing of 55% [*Marmer et al.*, 2007] for approximately the same time period.

[7] During the summer (June to September) a quasi-stationary upper anticyclone is extending over the eastern Mediterranean, causing sinking motion, thus, preventing any rising motion and precipitation [*Goldreich*, 2003; *Great Britain Meteorological Office*, 1962]. At the surface a low-pressure trough extends from the Persian Gulf through Iraq to the northeastern Mediterranean (Figure 1). Another quasi-stationary surface synoptic feature in summer is a high-pressure ridge extending from the Azore Islands over North Africa to the southeastern Mediterranean. These surface systems bring a regular, moist and relatively cool northwesterly flow over Israel capped by an elevated marine inversion. As a result of steep pressure gradient between the ridge in the northwest of the region and the Persian Trough in the southeast, northwesterly winds prevail throughout the entire season. These synoptic conditions cause long-range transport

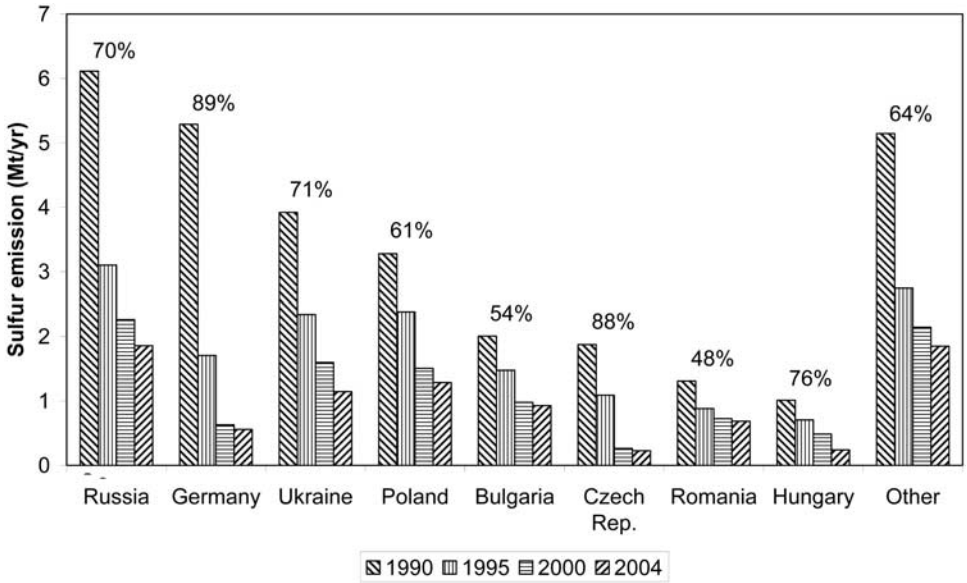

Figure 2. Temporal change of sulfur emission (mt a^{-1}) of the main polluted and other countries in central and eastern Europe in four key years: 1990, 1995, 2000, and 2004. (Data obtained from *Vestreng et al.* [2007]). The percentages indicate the percentage decrease in emissions in 2004 relative to 1990.

of air masses from southeastern and southwestern Europe, into the eastern Mediterranean basin. This low-level transport tends to carry pollution species along with it [*Dayan*, 1986; *Dayan and Levy*, 2005; *Erel et al.*, 2007; *Formenti et al.*, 2001a, 2001b; *Koch and Dayan*, 1992; *Luria et al.*, 1996; *Matvev et al.*, 2002; *Rudich et al.*, 2008; *Wanger et al.*, 2000]. The eastern Mediterranean is characterized by a stable marine boundary layer and sunny cloud-free days with little day-to-day variation. Any pollution transported to the region arrives undiluted with ample opportunity for photochemical reactions to enhance pollutant concentrations [*Kallos et al.*, 1993].

[8] In particular, it has been shown that transported air masses contain high levels of sulfate [*Luria et al.*, 1996; *Nativ et al.*, 1985; *Robinsohn et al.*, 1992]. *Luria et al.* [1996] measured the sulfate level for a 10-year period between 1984 and 1993, and found that the yearly mean sulfate concentration during the summer in Israel is as high as 500 nmol m^{-3} mostly due to transport from Europe. *Matvev et al.* [2002] found that during the summer and fall of 1998, the influx of sulfur arriving at the Israeli coast from Europe can be as high as 30 mg S h^{-1}. Using spaceborne data, *Rudich et al.* [2008] calculated sulfate flux for 2004 in a range of 0.025 to 0.062 Tg S a^{-1}. Note that outbreaks of mineral dust (which are in the coarse aerosol fraction) are not common during the summer [*Derimian et al.*, 2006].

[9] As introduced, a number of observations point to recent changes in sulfur emissions in both western and eastern Europe. Since these sulfate precursors are converted to aerosols, the distribution of these aerosols may also change. The objective of the current study is to verify that the temporal trend of reduction in SO_2 emissions in central and eastern Europe after 1991 results in a similar trend in sulfate levels in Israel as a receptor site. This hypothesis was examined by five long-term analyses of three independent data sets. The data sets include remote sensing measurements from space and ground, and in situ aerosol sampling. These data sets were analyzed for variability in aerosol optical thickness, size fractions, sampled mass concentrations, air mass backward trajectories, and calculated aerosol radiative forcing. The study was restricted to the summer season (July and August) thus only dry sulfate particles are involved rather than the removal of sulfate from the atmosphere by wet deposition.

[10] Temporal trends of atmospheric aerosols in general, and SO_2 in particular, might partially contribute to the global dimming versus global brightening debate. Ground-based measurements indicate that the amount of solar radiation reaching the Earth's surface decreased significantly during the 3 decades from 1960 to 1990 [*Stanhill and Cohen*, 2001]. The term "global dimming" was coined to describe this phenomenon. More recent surface as well as satellite observations suggest that this trend has reversed since 1990. A new term "global brightening" was invented in response [*Wild et al.*, 2005]. The reasons for these variations are not clear, but must be linked to changes in atmospheric properties such as clouds, aerosols, gases due to anthropogenic activities [*Alpert et al.*, 2005; *Alpert and Kishcha*, 2008], and not the sun, since solar irradiance variations are small compared to the observed dimming/brightening.

2. Methodology and Data Sets

2.1. Source and Receptor Areas

[11] Central and eastern Europe are considered the source area of the anthropogenic sulfate aerosols that are eventually observed in Israel. Several references of sulfur emission data sets are available with negligible differences: among them that of *Vestreng et al.* [2007] is the most updated one and includes data until 2004. Figure 2 presents the trends in emission from the main pollution producing countries. Note the high levels of emission declines in the Czech Republic

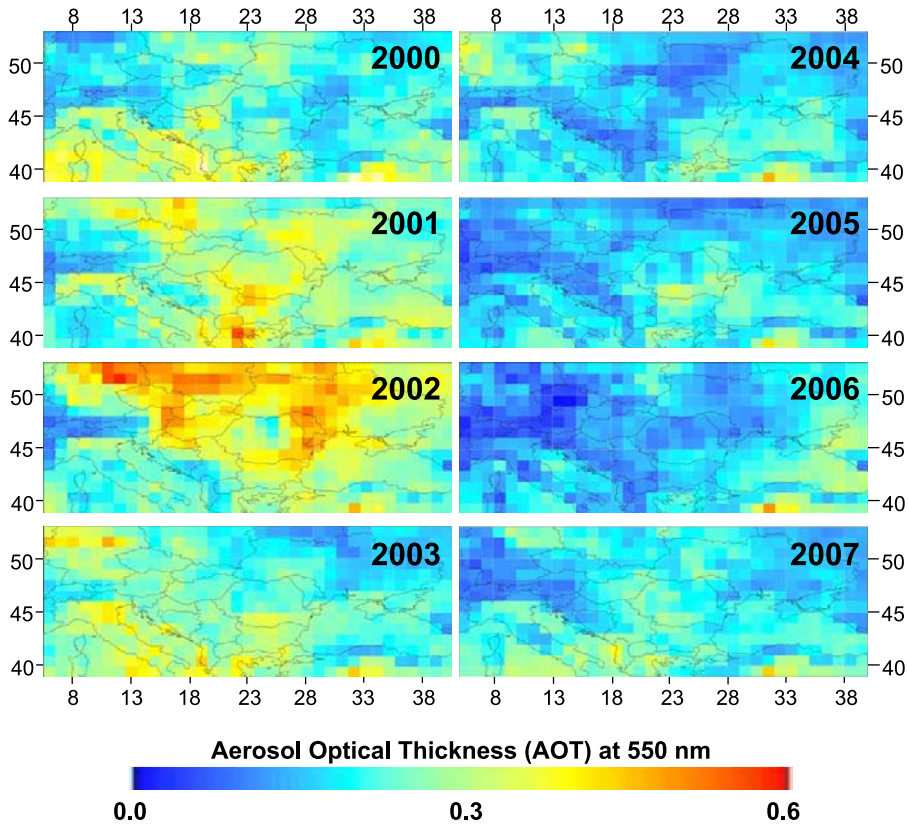

Figure 3. Spatial distribution (7°E–41°E; 40°N–53°N) and temporal variation (monthly means for July and August) of MODIS-Terra-derived total aerosol optical thickness (AOT) at 550 nm.

and Germany (88–89%) that were the main lignite producers prior to 1991.

[12] Sede Boker, which is located in the Negev desert, Israel (34°47′E, 30°51′N, 470 m above mean sea level), is a long-term station for investigating anthropogenic and natural aerosols in the eastern Mediterranean. Sede Boker was used to represent the receptor area of the European-generated aerosols. Optical properties of aerosols in Sede Boker were obtained from a sun/sky photometer (see below), while the aerosol chemical characteristics are acquired from a two-stage aerosol sampler (see below). Both instruments were operated almost continuously since 1995; however, the aerosol samplings were terminated in 2004.

2.2. Spaceborne Aerosol Optical Thickness

[13] Collection 5 (C005) "dark-target" aerosol products were derived from measured radiances observed by the Moderate Imaging Spectroradiometer (MODIS) aboard the Terra satellite between 2000 and 2007. The study focused specifically on monthly means of total aerosol optical thickness (AOT) and fine-sized AOT (fAOT), which is the fine particles contribution to the total AOT, for a latitude/longitude box between 7°E and 41°E and from 40°N to 53°N, covering central and eastern Europe and parts of the Mediterranean Sea (Figure 3). Theoretical and practical details of the algorithms for deriving aerosol products are found in several papers [*Kaufman et al.*, 1997; *Levy et al.*, 2007b; *Remer et al.*, 2005; *Tanre et al.*, 1997].

[14] In this study 10 km daily "dark target" retrievals were used to calculate monthly means for our region of interest, for both land and ocean. Only quality-assured (QA) retrievals are included in the monthly mean, and a minimum of five high QA retrievals are required in any given day for that day to be used to calculate the mean. The final result is pixel weighted, which tends to derive an average that is biased toward clear-sky values, but will be less affected by cloud artifacts in the retrieval. Directly retrieved parameters include total AOT (defined at 0.55 μm) and fine aerosol weighting (FW, also defined at 0.55 μm). Fine aerosol weighting is the ratio of fAOT to total AOT (fAOT = AOT $\times$ FW). The fAOT parameter has never been validated, but *Levy et al.* [2007b] demonstrated that it compares well to sunphotometer-derived fAOT over land, and it has been used in quantitative estimates of anthropogenic aerosol over ocean [e.g., *Kaufman et al.*, 2005].

2.3. Aerosol Optical Characteristics

[15] Aerosol optical properties were retrieved by a CIMEL sun/sky photometer (CE318, CIMEL Electronique, Paris, France) located at Sede Boker Campus of Ben Gurion University [*Derimian et al.*, 2006]. The instrument performs direct sun measurements every 15 min, with a 1.2° field of view at 340, 380, 440, 500, 675, 870, 940, and 1020 nm nominal wavelengths. The photometer belongs to a global network, named the Aerosol Robotic Network (AERONET) program, which includes hundreds of similar instruments all over the globe. The network is coordinated and maintained by the National Aeronautics and Space Administration

Table 1. Aerosol Optical Models and Calculated 24-h Average Top of Atmosphere Cloud-Free Aerosol Radiative Effect for the Central and Eastern European Source Region and the Israeli Receptor Site at the Beginning and End of Each Data Record[a]

	Europe 2000	Europe 2007	Israel 1998	Israel 2007
Fine AOT[b]	0.15	0.09	0.18	0.12
Fine SSA[b]	0.93	0.93	0.93	0.93
Fine asymmetry parameter[b]	0.66	0.66	0.66	0.66
Coarse AOT[b]	0.10	0.10	0.06	0.06
Coarse SSA[b]	0.95	0.95	0.95	0.95
Coarse asymmetry parameter[b]	0.70	0.70	0.70	0.70
Fine radiative effect (W m^{-2})[c]	−3.4	−1.7	−2.9	−1.3
Coarse radiative effect (W m^{-2})[c]	−2.2	−2.2	0.5	0.5
Total radiative effect (W m^{-2})[c]	−5.6	−3.9	−2.4	−0.8
Absolute difference of total radiative effect (W m^{-2})[c]	–	1.7	–	1.6
Difference of total radiative effect (%)	–	−30	–	−67

[a]Absolute and percent changes in flux are also indicated.
[b]Aerosol optical thickness (AOT), single scattering albedo (SSA), and asymmetry parameter are given for the midvisible wavelength range (553 nm) for both fine and coarse mode.
[c]Radiative effect in W m^{-2} represents 24-h average of the difference in net radiative flux at top of atmosphere between an atmosphere with aerosol and an atmosphere without. Negative radiative fluxes indicate planetary cooling.

(NASA) [*Holben et al.*, 1998]. The spectral AOT was obtained at seven of these wavelengths from direct sun measurements while the 940 nm channel was used to retrieve water vapor content. The angular distribution of sky radiance is also measured at 440, 670, 870, and 1020 nm. On the basis of these sun/sky photometer measurements the atmospheric aerosol size distributions, fine and coarse aerosol fractions, complex refractive indices, and other aerosol parameters are routinely retrieved using the AERONET inversion scheme [*Dubovik and King*, 2000]. This retrieval scheme was recently updated by considering a mixture of polydisperse, randomly oriented homogeneous spheroids with a fixed distribution of aspect ratios [*Mishchenko et al.*, 1997]. Another important update is usage of surface reflectance derived from satellite observation climatology [*Sinyuk et al.*, 2007]. More details on the retrieval algorithm and accuracy assessments can be found in the works by *Dubovik and King* [2000], *Dubovik et al.* [2000, 2002a, 2002b, 2006], and *Smirnov et al.* [2000]. For the current research, August data were used as a representative month of the summer season, during 10 years (1998–2007).

2.4. Aerosol Radiative Forcing

[16] The change in clear-sky direct aerosol radiative effect at the top of the atmosphere due to the decrease in AOT observed in both the source and receptor regions was calculated by the CLIRAD-SW solar radiative transfer code [*Chou*, 1992; *Chou and Suarez*, 1999]. Inputs to the radiative transfer computations include the fAOT and coarse AOT (cAOT), along with the corresponding single scattering albedo (SSA) and asymmetry parameter (assym). The summation of fAOT and cAOT is equal to the total AOT from the MODIS or the AERONET observations.

[17] The aerosol optical properties used in the radiative effect calculations were the same as assumed by the MODIS retrievals [*Levy et al.*, 2007a]. Note that SSA and assymetry parameter are assumed values and not retrieved by the satellite. The aerosol model for the fine model is described by *Levy et al.* [2007a] as the "moderate absorbing model," and the coarse mode is labeled "dust." Table 1 gives the midvisible (553 nm) values for the assumed optical properties. Each model's full spectral characteristics are described by *Levy et al.* [2007a].

[18] The aerosol effect for cloud-free conditions was calculated at the beginning of the study period (2000 in Europe; 1998 in Israel) and at the end (2007). The same aerosol characteristics were used for both Europe and Israel and for the beginning and end of the study period, but different mean noon time solar zenith angle (21° for Europe and 14.5° for Israel) and different surface albedos (0.15 for Europe and 0.22 for Israel) were used. It is expected that there is a change in chemical composition and resulting change in aerosol optical properties of the fine mode between the beginning and end of the study period, due to the obvious changes to European emissions. However, these changes were not taken into account when making the calculations. The primary purpose of these calculations is to illustrate the significance of the magnitude of change observed in the fine AOT, and not to present the "best possible estimate" of aerosol radiative forcing in the two regions of interest. For this purpose, the MODIS aerosol models applied constantly through the period are sufficient to illustrate the significance. Besides, these models have been applied constantly throughout the MODIS record, showing no change in the accuracy of the retrieval in eastern Europe, despite the changes in emissions.

[19] Radiative effect was computed only at the top of atmosphere and not at the surface because fluxes and forcing at the surface are highly dependent on aerosol absorption characteristics and SSA [*Remer and Kaufman*, 2006; *Satheesh and Ramanathan*, 2000]. Top of atmosphere fluxes and the MODIS aerosol retrieval are less sensitive. Without further information to constrain aerosol absorption properties during the study period, uncertainties of the surface forcing calculation are too large to be meaningful. The top of atmosphere calculations provide sufficient illustration.

2.5. Aerosol Chemical Characteristics

[20] A "Gent" PM10 Stacked Filter Unit (SFU) sampler was located at Sede Boker Campus and collected aerosol particles in coarse (2–10 μm aerodynamic diameter (AD)) and fine (<2 μm AD) size fractions [*Hopke et al.*, 1997; *Maenhaut et al.*, 1994]. The instrument was placed at about 8 m above the ground and operated at an airflow rate of ~12–16 L/min on a two-two-three-day scheme (with filter change on Sunday, Tuesday, and Thursday). Al-

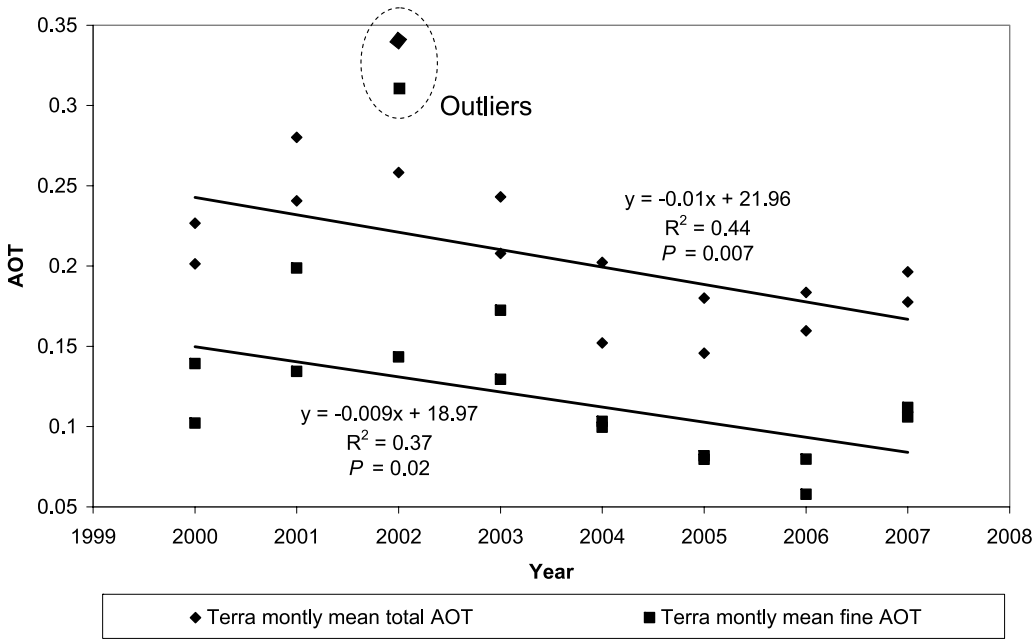

Figure 4. Temporal trend of AOT at 550 nm for July and August, derived from Terra-MODIS over the area in central and eastern Europe.

though the instrument worked continuously, to avoid the problem of filter clogging and thus nonrepresentative measurements, the sampling was always conducted with a timer set at 50% for the 2-day sample and at 33% for the 3-day sample; thus, the SFU effectively sampled only 50 or 33% of the time evenly distributed over 2 or 3 days, respectively. This resulted in little clogging or decrease in flow rate during the sampling, except during episodes with extremely large concentration. The SFU samples were analyzed for particulate mass (PM), black carbon, and over 40 elements at the Institute for Nuclear Sciences of Ghent University, Belgium. In this study, only the sulfur concentrations in the fine size fractions are presented with respect to the total fine and coarse PM concentration values. Sulfur was measured by particle-induced X-ray emission spectrometry (PIXE) [*Maenhaut and Cafmeyer*, 1998]. The instrument was operated continuously for 10 years from 1995 to 2004.

2.6. Air Mass Backward Trajectories

[21] The 5-day air mass backward trajectories were computed by the utility program HYSPBAT, part of the Trajectory Statistics (TS) software package [*Lupu and Maenhaut*, 2002]. HYSPBAT calculates backward air mass trajectories at a receptor site (Sede Boker Campus, in the current case) during a given period of time (1995–2004) by calling Hybrid Single-Particle Lagrangian Integrated Trajectory (HYSPLIT version 4 for PC) model of the National Oceanic and Atmospheric Administration (NOAA) [*Draxler and Hess*, 1998]. Calculations were performed for arrival at Sede Boker at 300 m above ground level and for a model domain up to 4000 m (and also up to 10,000 m) above ground level by using the global reanalysis meteorological data set. Consequently, origin of surface air mass and high-altitude long-range aerosol transport were obtained. Another utility program EXTRAJ, part of the TS software package, was used to extract and merge the calculated trajectories. Analyses were performed on all events with fine sulfur concentration above 3 μg m^{-3}. The image processing software, ERDAS-IMAGINE, was used to import ASCII files with these trajectories to ArcGis point coverage, which were overlaid together in a regional map.

3. Results and Discussion

3.1. Spaceborne AOT Characteristics at the Source Location

[22] Figure 4 shows both the total and fine monthly mean AOT at 550 nm for July and August, for the 8 years of Terra observations, and for the land-only box over Europe as shown in Figure 3. As one might notice, a high and significant correlation exists between the fAOT and the total AOT ($R^2 = 0.8$, $P < 0.001$). Therefore, isolating the submicron AOT from the total AOT at 550 nm reveals that the downward trend in aerosols over the past 8 years is driven by the decrease in small particles, either pollution or smoke. Summer 2002 shows up as anomalously high fine and total AOT values. During August 2002, notable peat fires and forest fires in the European part of the Russian Federation produced large quantities of smoke aerosol that was transported to neighboring countries [*Kovalev*, 2003]. Therefore, the August 2002 AOT values were excluded from the calculations of the reported regression trend lines and correlation coefficients. Figure 4 suggests that during the study period total AOT was declined by about 24% while the fine AOT by about 38%. It is also shown that at the beginning of the period fine AOT represented roughly

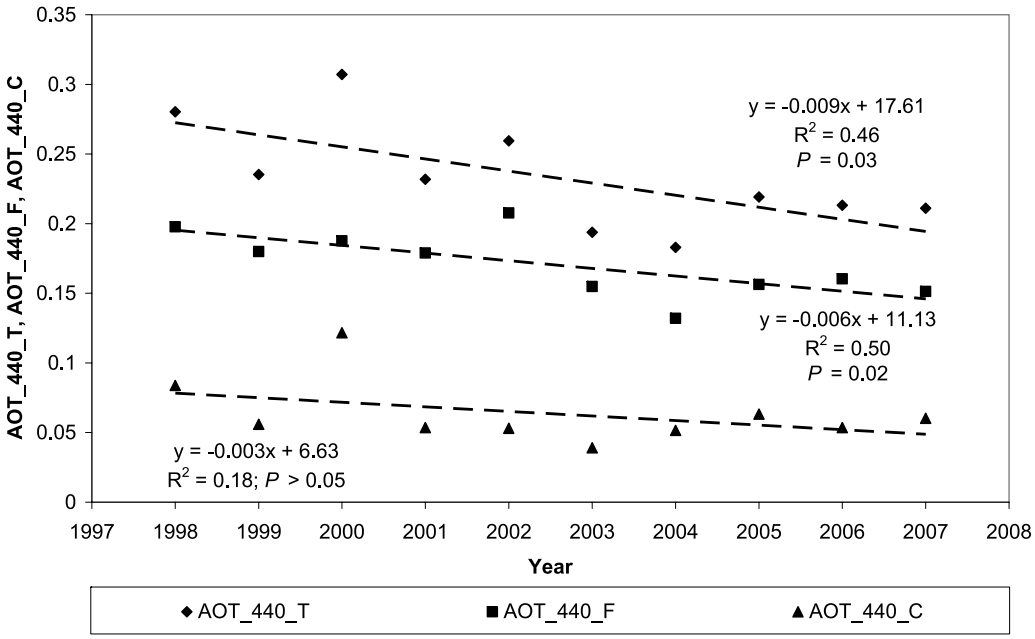

Figure 5. Temporal trend of total aerosol optical thickness at 440 nm, its fine and coarse fractions, for July and August, retrieved from the Sun photometer located at Sede Boker Campus, Israel. Observations of August 2002 were excluded owing to severe fires in eastern Europe.

60% of the total AOT, but at the end of the period only 50% of the total.

3.2. Aerosol Optical Characteristics at the Receptor Site

[23] Figure 5 shows the temporal trend of aerosol optical thickness, derived from AERONET observations, at 440 nm (AOT_440) in July and August between 1998 and 2007. The total AOT (AOT_440_T) is a linear summation of the AOT values caused by aerosols of the fine and coarse size fractions, which are products of the AERONET retrievals, and denoted in Figure 5 as AOT_440_F and AOT_440_C, respectively. As might be noticed, the coarse AOT values remain constant and relatively low, but the fine AOT and the total AOT values are very close and significantly correlated ($R^2 = 0.71$, $P = 0.002$). This indicates dominance of the fine aerosol fraction throughout the analyzed period. The year-to-year consistent dominance of the fine aerosol particles during August was also observed by *Derimian et al.* [2006]. Moreover, while the temporal dynamics of the coarse fraction AOT remains almost constant along the study period, the decline of the fine fraction is highly significant and its slope is identical to that for the total AOT values. In summary, the significant reduction of fine AOT by approximately 23% in July and August during 10 years of observations is interpreted as evidence of less anthropogenic air pollution reaching the receptor area as a function of time. Note that in August, the month during which Sede Boker is most dominated by pollution transport and least affected by dust [*Derimian et al.*, 2006], 43% reduction of fine AOT was observed. More variable aerosol type is expected for July; however, 2-month analysis was kept for consistency with the other data sets.

[24] Figure 6 shows the temporal trend of July–August mean SSA at 440 nm, obtained from the AERONET retrievals [*Dubovik and King*, 2000] between 1998 and 2007. Sufficient accuracy of SSA (~0.03) can be reached for an elevated aerosol loading (AOT_440 > 0.4), for specific geometrical conditions (solar zenith angle >50°), and only under cloud-free and homogeneous sky [*Dubovik and King*, 2000]. These stringent criteria reduce the number of data points in the July–August means, but maintain a higher reliability. In some months the monthly mean is composed of only a few points while in other months there were no retrievals to calculate a monthly mean. Unlike the total AOT, there is no discernible trend in the absorption characteristics of the aerosol at Sede Boker. This suggests that the composition of the aerosol affecting Sede Boker in July–August, while exhibiting interannual variability, is not linked to systematic changes in sulfur emissions. However, a definitive conclusion is prevented owing to a poor sampling statistic.

3.3. Aerosol Radiative Forcing Changes

[25] The decrease of AOT over both the source region and the receptor region introduces changes in the radiative balance in these two areas, but how significant are these changes? Are they 1%, 10%, or 100% changes to the aerosol radiative forcing? Providing a "best possible estimate" of the aerosol forcing changes is beyond the scope of this work. However, to put the observed aerosol changes into perspective, rough estimates of the consequences of the measured decreases were made, following the simplification of the problem described in section 2.4 above. The 40% decrease in fAOT in eastern Europe results in a 30% decrease in local aerosol radiative effect at top of atmosphere for cloud-free conditions, while a 35% decrease in fAOT over Israel introduces a 67% decrease in top of atmosphere radiative effect there. The exaggeration of the relative radiative effect in Israel is in part due to the brighter

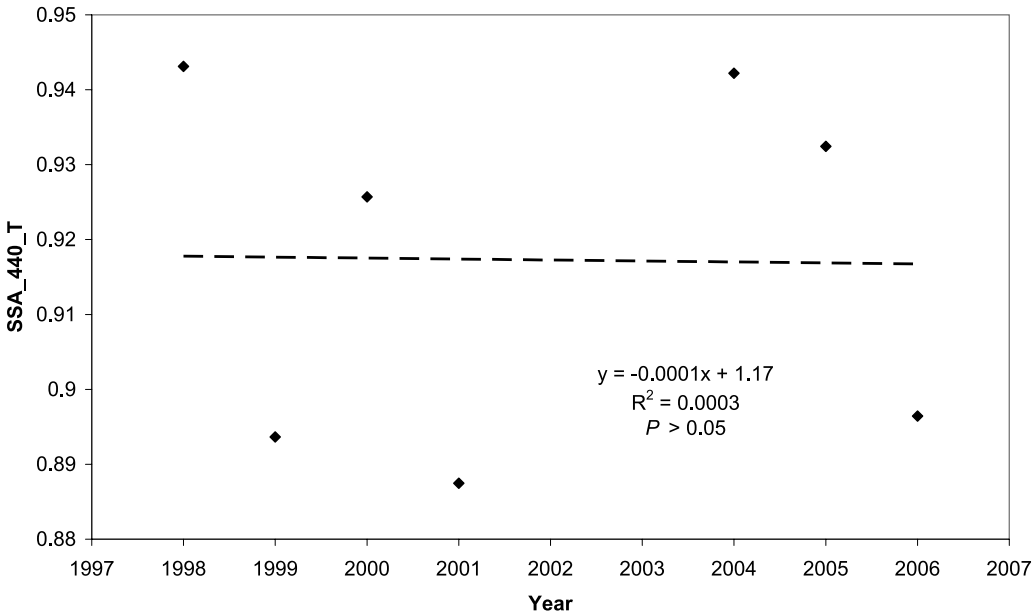

Figure 6. Temporal trend of July and August monthly mean total single scattering albedo (SSA) at 440 nm retrieved from the sun/sky photometer located at Sede Boker Campus, Israel.

surface albedo that lies near the critical reflectance value of the dust coarse mode [*Fraser and Kaufman*, 1985]. This neutralizes the top of atmosphere radiative effect of the coarse mode and accentuates the relative effects of the changes in the fine mode. The change in absolute flux is approximately the same in both regions. Table 1 lists the optical parameters and resulting top of atmosphere cloud-free aerosol forcing. All radiative flux values are 24-h averages [*Remer and Kaufman*, 2006].

[26] The year 2000 values of fine mode aerosol forcing over Europe from the current calculations (-3.4 W m^{-2}) is roughly three times larger than the values that *Marmer et al.* [2007] report for the same year. These authors are calculating forcing for sulfates only, while our calculations are for the total fine mode aerosol that contains a mix of aerosol particles including sulfates, organics, and even fine mode dust particles. Furthermore, the two study areas are different and in addition, *Marmer et al.* [2007] see a decrease in sulfate negative forcing of 1.5 W m^{-2} over a 20-year period, ending in 2000, while the current study calculates a change of 1.7 W m^{-2} in only 8 years, ending in 2007.

3.4. Aerosol Chemical Characteristics at the Receptor

[27] Since the AERONET data can distinguish only between the fine and coarse fractions of AOT and suggest a SSA for the total aerosol, ground sampling of aerosols in these two fractions followed by chemical analyses are needed to verify the above findings and to point to the elements involved. Figure 7a shows an insignificant trend of the total coarse PM concentration that represents mainly mineral dust in the study area [*Derimian et al.*, 2006] for the summer months (July and August), along the 10 sampling years. A statistical significant decrease, however, of the total fine PM concentration is obtained throughout the study years (Figure 7b). Especially the concentration of fine sulfur (which is essentially fine non sea-salt sulfur) shows a highly significant decline (Figure 7c). A notable decrease of approximately 24% can be observed along the study years. As indicated above, the fine fraction of sulfur is indicative to anthropogenic air pollution, in contrast to sulfur in the coarse fraction which has a substantial contribution from sea salt.

3.5. Connecting Receptor and Source by Air Mass Backward Trajectories

[28] Air mass backward trajectories link receptor and source areas. The method used is based on combining chemical data, sulfur in the current case, with the calculated trajectories. As noted before, the lifetime of sulfur in the atmosphere ranges from 12 h to 6 days. Therefore, 5-day air mass backward trajectories from the receptor site at Sede Boker and during July and August, and along the 10 years of aerosol samplings (1995–2004) are overlaid (Figure 8). These trajectories represent extreme events in which the fine fraction sulfur concentration at the receptor exceeded a threshold of 3 μg m^{-3}. A total of 75 such events are presented. While 0 to 15 events occurred each summer, their number is significantly reduced along the study years (Figure 9). As can be seen in Figure 8, the majority of the calculated trajectories are heading northwest from the receptor site. This finding agrees well the general synoptic circulation of the eastern Mediterranean during the summer, as previously discussed. The majority of the events (60%) are originated from Russia, Ukraine, and northern Black Sea region, 26% from the southern Mediterranean countries (Turkey, Italy, and Greece), and 8% are originated in the Eastern Europe. It is estimated that if longer backward trajectory analysis were applied, more trajectories would start in northern areas.

4. Summary and Conclusions

[29] Reduction of sulfur emissions over central and eastern Europe after the collapse of the Soviet Bloc in 1991 is well

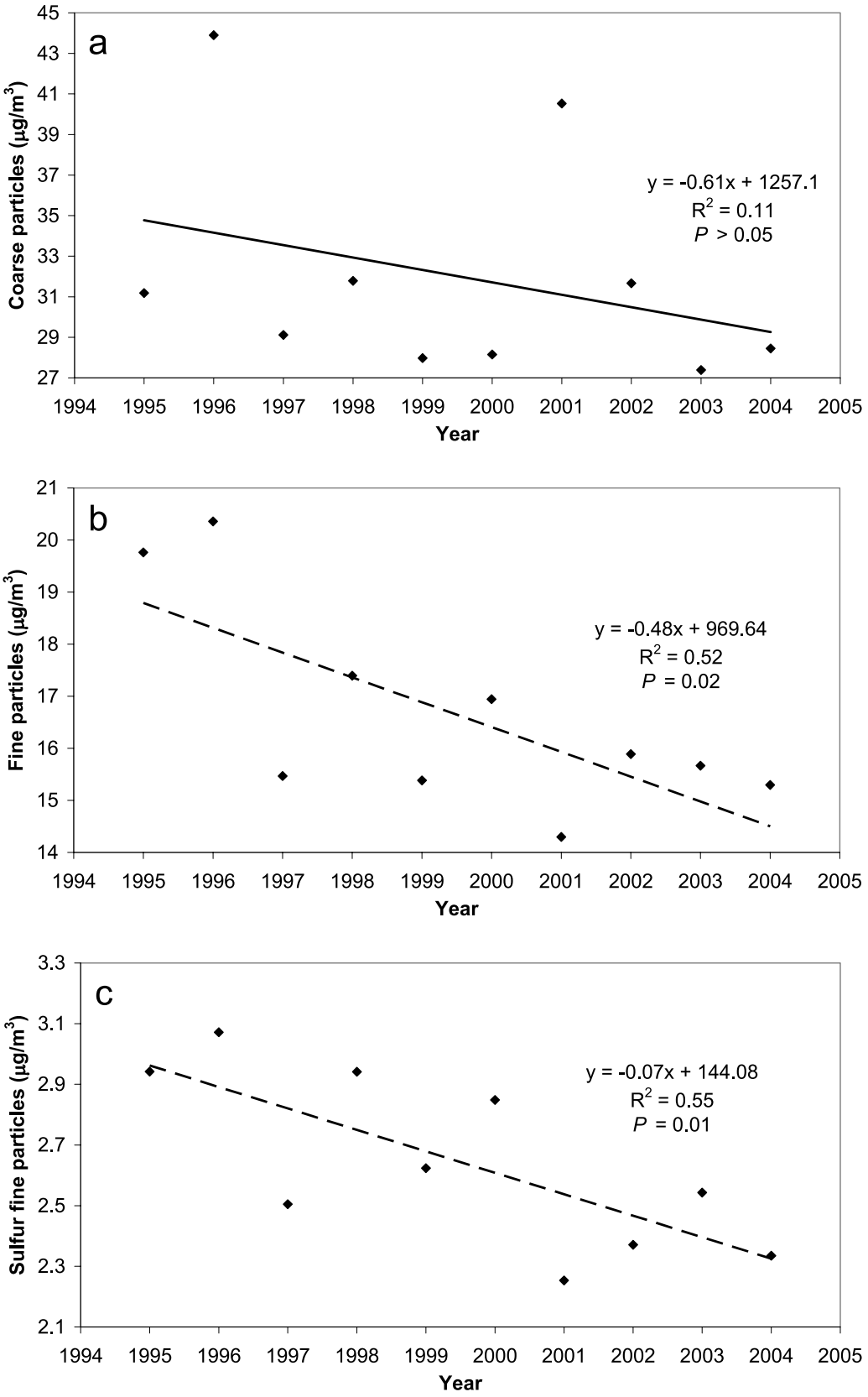

Figure 7. Temporal trends of mass concentrations for July and August, obtained from a two-stage aerosol sampler located at Sede Boker Campus: (a) coarse particles, (b) fine particles, (c) fine sulfur.

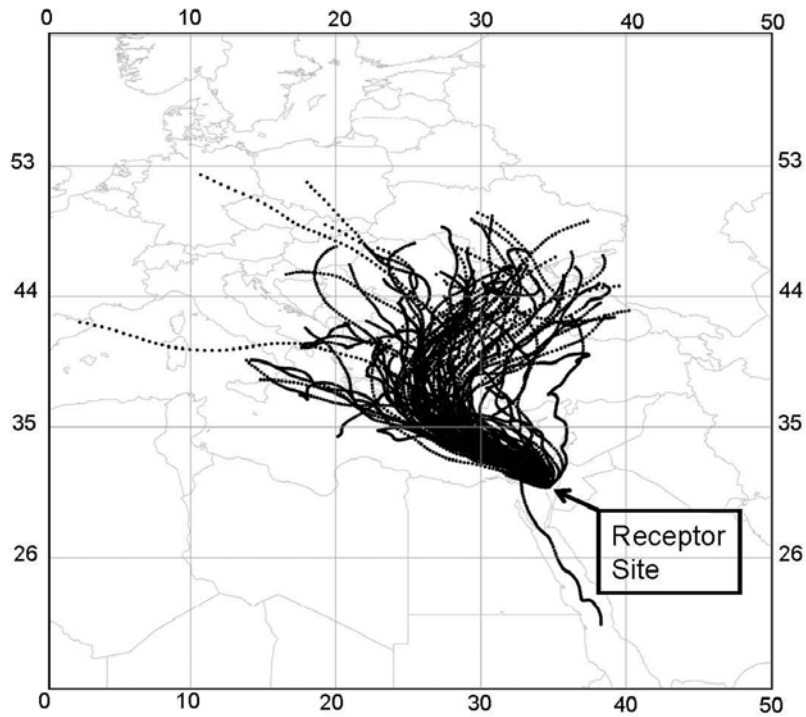

Figure 8. Five-day air mass backward trajectories from Sede Boker Campus. Trajectories are applied to arrival height of 300 m above ground level and relate only to events when the fine sulfur concentration exceeded 3 μg m^{-3} in July and August and along the 10 years of aerosol samplings (1995–2004). The majority of the 75 presented trajectories are originated from eastern and central Europe.

observed and documented. The main reasons are sharp decrease in economic activities and energy production, emission control and the adaptation to western European standards, and changes in fuel supply. The current research indicates that this gradual change influenced a site located thousands of kilometers downwind. Two remote sensing data sets, one with spaceborne data, derived from the Terra-MODIS aerosol product over the source area, and the other with ground optical data, by means of Sun photometer at the receptor area, strengthened the research hypothesis and showed a significant reduction of fine aerosols of 38% and 43%, respectively. However, both remote sensing instruments provide data on suspended aerosols and can distinguish between fine and coarse particles but are limited in analyzing their composition. In order to derive specific information on fine non sea-salt sulfur, a two-stage aerosol

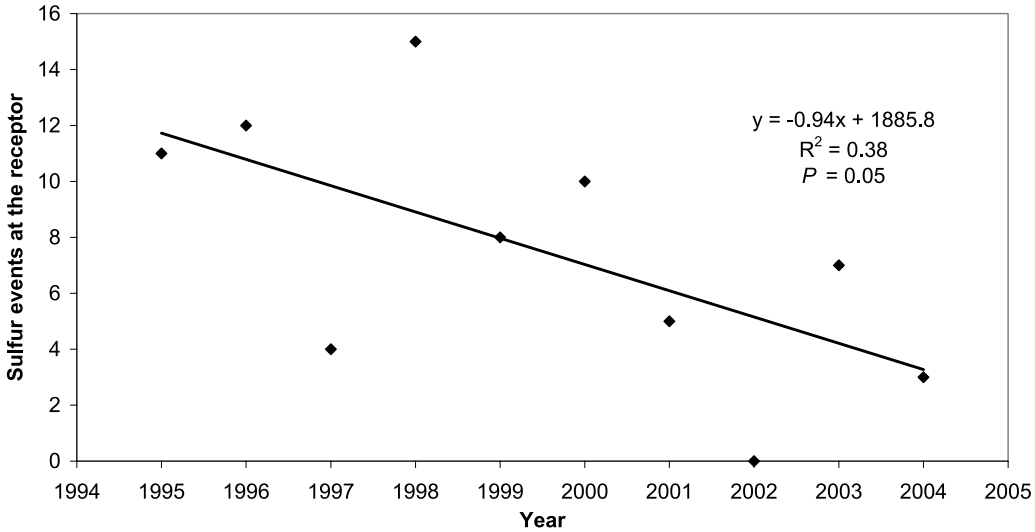

Figure 9. Temporal trend of number of events, in July and August, in which fine fraction sulfur concentration at the receptor exceeded a threshold of 3 μg m^{-3}.

sampler was used, together with an appropriate chemical analysis. This data set independently confirmed the remote sensing observations and showed a significant reduction of the fine sulfur levels. Air mass backward trajectories were used to link the source and the receptor areas.

[30] The receptor site, located in the central Negev desert, showed definite decrease in fine sulfur aerosols. It should be noted that these observations are in contradiction to the fact that the population of Israel increased in the parallel period by 53%, from 4.7 million in 1990 to 7.2 million at the end of 2007, mainly owing to a large wave of immigration from the former Soviet Union countries. This growth was followed by a parallel increase of all types of economic activities. According to the EDGAR database (http://www.mnp.nl/edgar) the sulfur emission from Israel increased by 60% between 1990 and 2000. Power plants, located along the Israeli Mediterranean coast, only 100 to 200 km away from the Sede Boker Campus, are the main source (about 65%) of sulfur emission in Israel (http://www.mnp.nl/edgar). Nevertheless, owing to the synoptic meteorological conditions of the region during the summer, i.e., shallow boundary layer and weak winds that prevent local air pollution buildup along with steep pressure gradient between the ridge in the northwest of the region and the Persian Trough in the southeast, Sede Boker remains unaffected by this local increase in pollution, and remains an appropriate reference site to examine pollution aerosols, transported thousands of kilometers downwind from their origin.

[31] Since the SO_x aerosols play a major role in anthropogenic direct and indirect climate forcing, they have received a considerable attention over the past decade. Numerous studies were dedicated to the impacts of the fine aerosol fraction, and the SO_x aerosols in particular, on the Earth radiative budget. Consequently, monitoring the temporal dynamics of anthropogenic sulfur aerosol might explain fundamental issues in understanding and predicting climate change processes. In particular, the current study highlights the complexity of the problem. Changes in emissions in one region can produce local changes in radiative effect, but these emission trends may have different consequences downwind at receptor sites where different surface albedo, solar geometry, and background aerosol can either accentuate or mitigate the radiative impact. The current study indicates a 67% decrease in aerosol cooling over Israel, which may influence regional mesoscale circulations and weather patterns.

[32] Since the ground-based and spaceborne remote sensing observations, the in situ aerosol sampling, and the aerosol radiative forcing calculations indicate consistent decrease in AOT and fine aerosols concentrations, the study findings support the global brightening theory reported since 1990. The study confirms that the dramatic turnover from dimming to brightening is dominated by the anthropogenic/economic activities. However, although several studies [e.g., *Alpert et al.*, 2005; *Alpert and Kishcha*, 2008] claim that the dimming and brightening phenomena are of local or regional nature, restricted to large urbanized and highly populated sites, the current study demonstrates that aerosol effects can have a long-range influence and are not just of local importance.

[33] **Acknowledgments.** The research was partially funded by the Israeli Ministry of Environmental Protection. The authors wish to thank A. Zangvil for the synoptic description and map and acknowledge research support from the Belgian Federal Science Policy Office and the Special Research Fund of Ghent University.

References

Alpert, P., and P. Kishcha (2008), Quantification of the effect of urbanization on solar dimming, *Geophys. Res. Lett.*, *35*, L08801, doi:10.1029/2007GL033012.

Alpert, P., et al. (2005), Global dimming or local dimming?: Effect of urbanization on sunlight availability, *Geophys. Res. Lett.*, *32*, L17802, doi:10.1029/2005GL023320.

Andreae, M. O., and D. Rosenfeld (2008), Aerosol-cloud-precipitation interactions. Part 1. The nature and sources of cloud-active aerosols, *Earth Sci. Rev.*, *89*, 13–41, doi:10.1016/j.earscirev.2008.03.001.

Chin, M. A., and D. J. Jacob (1996), Anthropogenic and natural contributions to tropospheric sulfate: A global model analysis, *J. Geophys. Res.*, *101*(D13), 18,691–18,699, doi:10.1029/96JD01222.

Chin, M., et al. (2000), Atmospheric sulfur cycle simulated in the global model GOCART: Model description and global properties, *J. Geophys. Res.*, *105*(D20), 24,671–24,687, doi:10.1029/2000JD900384.

Chou, M.-D. (1992), A solar-radiation model for use in climate studies, *J. Atmos. Sci.*, *49*(9), 762–772, doi:10.1175/1520-0469(1992)049<0762:ASRMFU>2.0.CO;2.

Chou, M.-D., and M. J. Suarez (1999), A solar radiation parameterization (CLIRAD-SW) for atmospheric studies, *NASA Tech. Memo., 10460*, 48 pp.

Dayan, U. (1986), Climatology of back trajectories from Israel based on synoptic analysis, *J. Clim. Appl. Meteorol.*, *25*(5), 591–595, doi:10.1175/1520-0450(1986)025<0591:COBTFI>2.0.CO;2.

Dayan, U., and I. Levy (2005), The influence of meteorological conditions and atmospheric circulation types on PM10 and visibility in Tel Aviv, *J. Appl. Meteorol.*, *44*(5), 606–619, doi:10.1175/JAM2232.1.

Derimian, Y., et al. (2006), Dust and pollution aerosols over the Negev desert, Israel: Properties, transport, and radiative effect, *J. Geophys. Res.*, *111*, D05205, doi:10.1029/2005JD006549.

Draxler, R. R., and G. D. Hess (1998), An overview of the Hysplit_4 Modeling System for Trajectories, *Aust. Meteorol. Mag.*, *47*, 295–308.

Dubovik, O., and M. D. King (2000), A flexible inversion algorithm for retrieval of aerosol optical properties from Sun and sky radiance measurements, *J. Geophys. Res.*, *105*(D16), 20,673–20,696, doi:10.1029/2000JD900282.

Dubovik, O., et al. (2000), Accuracy assessments of aerosol optical properties retrieved from Aerosol Robotic Network (AERONET) Sun and sky radiance measurements, *J. Geophys. Res.*, *105*(D8), 9791–9806, doi:10.1029/2000JD900040.

Dubovik, O., et al. (2002a), Variability of absorption and optical properties of key aerosol types observed in worldwide locations, *J. Atmos. Sci.*, *59*(3), 590–608, doi:10.1175/1520-0469(2002)059<0590:VOAAOP>2.0.CO;2.

Dubovik, O., et al. (2002b), Non-spherical aerosol retrieval method employing light scattering by spheroids, *Geophys. Res. Lett.*, *29*(10), 1415, doi:10.1029/2001GL014506.

Dubovik, O., et al. (2006), Application of spheroid models to account for aerosol particle nonsphericity in remote sensing of desert dust, *J. Geophys. Res.*, *111*, D11208, doi:10.1029/2005JD006619.

Erel, Y., et al. (2007), European atmospheric pollution imported by cooler air masses to the eastern Mediterranean during the summer, *Environ. Sci. Technol.*, *41*(15), 5198–5203, doi:10.1021/es062247n.

Formenti, P., et al. (2001a), Aerosol optical properties and large-scale transport of air masses: Observations at a coastal and a semiarid site in the eastern Mediterranean during summer 1998, *J. Geophys. Res.*, *106*(D9), 9807–9826, doi:10.1029/2000JD900609.

Formenti, P., et al. (2001b), Physical and chemical characteristics of aerosols over the Negev desert (Israel) during summer 1996, *J. Geophys. Res.*, *106*(D5), 4871–4890, doi:10.1029/2000JD900556.

Fraser, R. S., and Y. J. Kaufman (1985), The relative importance of aerosol scattering and absorption in remote-sensing, *IEEE Trans. Geosci. Remote Sens.*, *GE-23*(5), 625–633, doi:10.1109/TGRS.1985.289380.

Goldreich, Y. (2003), *The Climate of Israel: Observation, Research and Applications*, 270 pp.Kluwer Acad., New York.

Great Britain Meteorological Office (1962), *Weather in the Mediterranean*, 2nd ed., 362 pp., London.

Holben, B. N., et al. (1998), AERONET: A federated instrument network and data archive for aerosol characterization, *Remote Sens. Environ.*, *66*(1), 1–16, doi:10.1016/S0034-4257(98)00031-5.

Hopke, P. K., et al. (1997), Characterization of the Gent stacked filter unit PM10 sampler, *Aerosol Sci. Technol.*, *27*(6), 726–735, doi:10.1080/02786829708965507.

Kallos, G., et al. (1993), Synoptic and mesoscale weather conditions during air-pollution episodes in Athens, Greece, *Boundary Layer Meteorol.*, *62*(1–4), 163–184, doi:10.1007/BF00705553.

Kaufman, Y. J., et al. (1997), Operational remote sensing of tropospheric aerosol over land from EOS moderate resolution imaging spectroradiometer, *J. Geophys. Res.*, *102*(D14), 17,051–17,067, doi:10.1029/96JD03988.

Kaufman, Y. J., et al. (2005), Aerosol anthropogenic component estimated from satellite data, *Geophys. Res. Lett.*, *32*, L17804, doi:10.1029/2005GL023125.

Kellogg, W. W., et al. (1972), Sulfur cycle, *Science*, *175*(4022), 587–596, doi:10.1126/science.175.4022.587.

Koch, J., and U. Dayan (1992), A synoptic analysis of the meteorological conditions affecting dispersion of pollutants emitted from tall stacks in the coastal-plain of Israel, *Atmos. Environ., Part A*, *26*(14), 2537–2543.

Kovalev, N. A. (2003), *Russian Federation Fire 2002 Special. Part I. The wildland fire season 2002 in the Russian Federation. An assessment by the Global Fire Monitoring Center*, 34 pp., Global Fire Monit. Cent., Freiburg, Germany.

Levy, R. C., L. A. Remer, and O. Dubovik (2007a), Global aerosol optical properties and application to Moderate Resolution Imaging Spectroradiometer aerosol retrieval over land, *J. Geophys. Res.*, *112*, D13210, doi:10.1029/2006JD007815.

Levy, R. C., L. A. Remer, S. Mattoo, E. F. Vermote, and Y. J. Kaufman (2007b), Second-generation operational algorithm: Retrieval of aerosol properties over land from inversion of Moderate Resolution Imaging Spectroradiometer spectral reflectance, *J. Geophys. Res.*, *112*, D13211, doi:10.1029/2006JD007811.

Lupu, A., and W. Maenhaut (2002), Application and comparison of two statistical trajectory techniques for identification of source regions of atmospheric aerosol species, *Atmos. Environ.*, *36*(36–37), 5607–5618, doi:10.1016/S1352-2310(02)00697-0.

Luria, M., et al. (1996), Atmospheric sulfur over the east Mediterranean region, *J. Geophys. Res.*, *101*(D20), 25,917–25,930, doi:10.1029/96JD01579.

Maenhaut, W., and J. Cafmeyer (1998), Long-term atmospheric aerosol study at urban and rural sites in Belgium using multi-elemental analysis by particle-induced X-ray emission spectrometry and short-irradiation instrumental neutron activation analysis, *X Ray Spectrom.*, *27*(4), 236–246, doi:10.1002/(SICI)1097-4539(199807/08)27:4<236::AID-XRS292>3.0.CO;2-F.

Maenhaut, W., F. François, and J. Cafmeyer (1994), The "Gent" stacked filter unit (SFU) sampler for the collection of aerosols in two size fractions: Description and instructions for installation and use, in *Applied Research on Air Pollution Using Nuclear-Related Analytical Techniques: Report on the First Research Co-ordination Meeting, Vienna, Austria, 30 March–2 April 1993*, pp. 249–263, IAEA, Vienna.

Marmer, E., et al. (2007), Direct shortwave radiative forcing of sulfate aerosol over Europe from 1900 to 2000, *J. Geophys. Res.*, *112*, D23S17, doi:10.1029/2006JD008037.

Matvev, V., et al. (2002), Atmospheric sulfur flux rates to and from Israel, *Sci. Total Environ.*, *291*(1–3), 143–154, doi:10.1016/S0048-9697(01)01089-0.

Meagher, J. F., et al. (1983), The seasonal-variation of the atmospheric SO_2 to SO_4^{2-} conversion rate, *J. Geophys. Res.*, *88*(C2), 1525–1527, doi:10.1029/JC088iC02p01525.

Mishchenko, M. I., et al. (1997), Modeling phase functions for dustlike tropospheric aerosols using a shape mixture of randomly oriented polydisperse spheroids, *J. Geophys. Res.*, *102*(D14), 16,831–16,847, doi:10.1029/96JD02110.

Myhre, G., et al. (2004), The radiative effect of the anthropogenic influence on the stratospheric sulfate aerosol layer, *Tellus, Ser. B*, *56*(3), 294–299, doi:10.1111/j.1600-0889.2004.00106.x.

Mylona, S. (1996), Sulphur dioxide emissions in Europe 1880–1991 and their effect on sulphur concentrations and depositions, *Tellus, Ser. B*, *48*(5), 662–689, doi:10.1034/j.1600-0889.1996.t01-2-00005.x.

Nativ, R., et al. (1985), The occurrence of sulfate-rich rains in the Negev desert, Israel, *Tellus, Ser. B*, *37*(3), 166–172.

Remer, L. A., and Y. J. Kaufman (2006), Aerosol direct radiative effect at the top of the atmosphere over cloud free ocean derived from four years of MODIS data, *Atmos. Chem. Phys.*, *6*, 237–253.

Remer, L. A., et al. (2005), The MODIS aerosol algorithm, products, and validation, *J. Atmos. Sci.*, *62*(4), 947–973, doi:10.1175/JAS3385.1.

Robinsohn, J., et al. (1992), The effects of mesoscale circulation on the dispersion of pollutants (SO_2) in the eastern Mediterranean, southern coastal-plain of Israel, *Atmos. Environ., Part B*, *26*(3), 271–277, doi:10.1016/0957-1272(92)90002-A.

Rudich, Y., et al. (2008), Estimation of transboundary transport of pollution aerosols by remote sensing in the eastern Mediterranean, *J. Geophys. Res.*, *113*, D14S13, doi:10.1029/2007JD009601.

Satheesh, S. K., and V. Ramanathan (2000), Large differences in tropical aerosol forcing at the top of the atmosphere and Earth's surface, *Nature*, *405*(6782), 60–63, doi:10.1038/35011039.

Sinyuk, A., et al. (2007), Simultaneous retrieval of aerosol and surface properties from a combination of AERONET and satellite data, *Remote Sens. Environ.*, *107*(1–2), 90–108, doi:10.1016/j.rse.2006.07.022.

Smirnov, A., et al. (2000), Cloud-screening and quality control algorithms for the AERONET database, *Remote Sens. Environ.*, *73*(3), 337–349, doi:10.1016/S0034-4257(00)00109-7.

Stanhill, G., and S. Cohen (2001), Global dimming: A review of the evidence for a widespread and significant reduction in global radiation with discussion of its probable causes and possible agricultural consequences, *Agric. For. Meteorol.*, *107*(4), 255–278, doi:10.1016/S0168-1923(00)00241-0.

Stockwell, W. R., and J. G. Calvert (1983), The mechanism of the HO-SO_2 reaction, *Atmos. Environ.*, *17*(11), 2231–2235, doi:10.1016/0004-6981(83)90220-2.

Tanre, D., et al. (1997), Remote sensing of aerosol properties over oceans using the MODIS/EOS spectral radiances, *J. Geophys. Res.*, *102*(D14), 16,971–16,988, doi:10.1029/96JD03437.

Vestreng, V., et al. (2007), Twenty-five years of continuous sulphur dioxide emission reduction in Europe, *Atmos. Chem. Phys.*, *7*, 3663–3681.

Wanger, A., et al. (2000), Some observational and modeling evidence of long-range transport of air pollutants from Europe toward the Israeli coast, *J. Geophys. Res.*, *105*(D6), 7177–7186, doi:10.1029/1999JD901060.

Wild, M., et al. (2005), From dimming to brightening: Decadal changes in solar radiation at Earth's surface, *Science*, *308*(5723), 847–850, doi:10.1126/science.1103215.

Y. Derimian, Laboratoire d'Optique Atmosphérique, Université de Lille 1/CNRS, Villeneuve d'Ascq F-59655, France.

B. N. Holben, R. C. Levy, and L. A. Remer, NASA Goddard Space Flight Center, Greenbelt, MD 20771, USA.

R. Indoitu, A. Karnieli, and N. Panov, Remote Sensing Laboratory, Jacob Blaustein Institutes for Desert Research, Ben-Gurion University of the Negev, Sede Boker Campus 84990, Israel. (karnieli@bgu.ac.il)

W. Maenhaut, Department of Analytical Chemistry, Institute for Nuclear Sciences, Ghent University, Gent B-9000, Belgium.